

## THEORY OF PARAMETRIC EXCITATION OF ACOUSTIC WAVES

A. R. Muratov

*Institute for Oil and Gas Research, Russian Academy of Sciences  
117917, Moscow, Russia  
Department of Physics, Weizmann Institute of Science  
76100, Rehovot, Israel*

Submitted May 26, 1997

A theory of parametric excitation of acoustic waves is constructed. It is shown that nonlinear attenuation is the main restriction mechanism for a parametrically generated sound wave. The intensity of generated waves is directly proportional to the difference  $\epsilon$  between the value of pumping and bare attenuation. The calculated proportionality coefficient depends on the shape of the generated sound wave. Why an ordinary pattern does not form for acoustical waves is explained. The structure of the spectrum of excited waves was studied. It is shown that this structure has exponential asymptotic behavior at the frequency. The width of the intensity distribution depends on the shape of a wave. For different cases it behaves as  $\epsilon^\alpha$  with  $\alpha = 1, 8/7, \text{ and } 4/3$ . The results are compared with the experimental data of Ref. [5].

## 1. INTRODUCTION

Parametric excitation of waves is observed in a wide class of dynamical systems for waves with different dispersion relations [1]. These dispersion relations can be divided into two groups: nondecaying and decaying. As an example from the first group we have spin waves and from the second group waves on the free surface of a liquid. For spin waves conservation laws of frequency and wave vector, as a rule, do not permit three-wave interactions. The behavior of spin-wave systems in those cases is determined by four-wave interactions. The corresponding theory is well developed and is described elsewhere [2, 3]. The main mechanism for saturation of the amplitude of generated wave in these systems is the so-called dephasing mechanism, i.e., renormalization of the pumping due to the interaction between secondary waves. Capillary waves on the free surface of a liquid have the dispersion relation  $\omega \propto k^{3/2}$ , where  $\omega$  is the frequency and  $k$  is the wave vector of the wave. Three-wave interaction is allowed for this dispersion relation. The pattern selection and amplitude saturation for surface waves are determined by a nonlinear attenuation, as has been shown in Ref. [4].

The case of acoustic dispersion relation  $\omega \propto k$  is the marginal case between these two possibilities. In this case the conservation laws allow three-wave interactions but only for the waves with collinear (parallel or antiparallel) wave vectors. This case, which we will consider in this paper, was not studied at all. We will show that nonlinear attenuation is the main mechanism for restriction of amplitude of a parametrically generated sound wave. The intensity of generated waves is directly proportional to the difference between the value of pumping and the bare attenuation. The proportionality coefficient depends on the shape of the excited sound wave.

Three-wave interaction of sound waves is allowed only if their wave vectors are almost collinear. This special interaction destroys the long-range order at an angle between the

directions of propagation of waves; therefore, ordinary pattern formation does not occur in the case of acoustical waves. We will find the fine structure of the spectrum of generated waves. It turns out that it has exponential asymptotic behavior at the frequency which is known for the other nonlinear systems [3]. The behavior of the width of the spectrum for acoustical waves differs from the one known for spin waves. The width of the intensity distribution depends on the shape of the wave. For different cases it behaves as  $\epsilon^\alpha$  with  $\alpha = 1, 8/7,$  and  $4/3$ . The results of this paper were compared with many data obtained in experiments with parametric excitation of the second-sound waves in liquid helium by the first-sound wave [5, 6]. We obtained good qualitative and quantitative agreement with the experimental results.

## 2. THE EFFECTIVE ACTION

It is suitable to use Hamiltonian approach to describe nonlinear dynamics of waves. It is not a simple problem to find the corresponding canonical variables in general [3, 7]. We will assume that this problem has already been solved. For the dynamics of liquid helium the canonical variables were found in Ref. [8]. In canonical variables the Hamiltonian of a system can be written as

$$H = \int d^3r \left( b^*(t, \mathbf{r})\omega(\nabla)b(t, \mathbf{r}) + U[a^*(t, \mathbf{r})b(t, \mathbf{r})b(t, \mathbf{r}) + \text{c.c.}] + V[b^*(t, \mathbf{r})b(t, \mathbf{r})b(t, \mathbf{r}) + \text{c.c.}] \right). \tag{1}$$

Here  $b(t, \mathbf{r})$  is the wave variable which describes the excited sound wave,  $\omega = c\sqrt{-\nabla^2}$  is its dispersion relation, and  $c$  is the phase velocity of the sound wave. We will study parametric excitation of the sound wave  $b(t, \mathbf{r})$  by the external wave field  $a(t, \mathbf{r})$  (pumping wave). The parameter  $U$  in Eq. (1) is the vertex of the three-wave interaction of the pumping wave and the excited waves, and  $V$  is the vertex of the three-wave self-interaction.

Equation (1) is simply an expansion over the value of the excited wave; it can be used only if the amplitude of the excited wave is small, i.e., not far from the excitation threshold. In general, we can prolong expansion (1) and take into account four-wave interaction of the excited waves. It is necessary if the three-wave interaction is not allowed due to the conservation laws of frequency and wave vector. As will be shown below, for the sound waves we can consider only the three-wave interaction.

It is useful to make Fourier transform of the wave field:

$$b(t, \mathbf{r}) = \int \frac{d^3k}{(2\pi)^3} b(t, \mathbf{k})e^{i\mathbf{k}\mathbf{r}}. \tag{2}$$

We can then write the Hamiltonian as

$$H = \int \frac{d^3k}{(2\pi)^3} \left[ \omega(k)b(\mathbf{k})b^*(\mathbf{k}) + \int \frac{d^3q}{(2\pi)^3} \left( U(\mathbf{k}, \mathbf{q})[a^*(\mathbf{k})b(\mathbf{q})b(\mathbf{k} - \mathbf{q}) + \text{c.c.}] + V(\mathbf{k}, \mathbf{q})[b^*(\mathbf{k})b(\mathbf{q})b(\mathbf{k} - \mathbf{q}) + \text{c.c.}] \right) \right]. \tag{3}$$

Here  $\omega$  and  $\mathbf{k}$  are the frequency and the wave vector of the sound wave, and  $\omega(k)$  is its dispersion relation. The expansion in (3) is an ordinary hydrodynamic expansion and its parameter is  $\sqrt{\omega}b$ . It means that the vertices  $U$  and  $V$  are proportional to

$$\sqrt{\omega(k_1)\omega(k_2)\omega(k_3)}. \tag{4}$$

We will use complex canonical variables, in which the dynamical equations have the form

$$i\partial_t b(\mathbf{k}) = \frac{\delta H}{\delta b^*(\mathbf{k})}, \quad -i\partial_t b^*(\mathbf{k}) = \frac{\delta H}{\delta b(\mathbf{k})}. \tag{5}$$

In our case we have

$$i\partial_t b(\mathbf{k}) = \omega(k)b(\mathbf{k}) + \int \frac{d^3q}{(2\pi)^3} \left( 2Ua(\mathbf{k} + \mathbf{q})b^*(\mathbf{q}) + V[2b(\mathbf{q})b^*(\mathbf{q} - \mathbf{k}) + b(\mathbf{q})b(\mathbf{k} - \mathbf{q})] \right). \tag{6}$$

The second equation is a complex conjugated equation (6).

Equation (6) is a conservative equation to which a dissipative term must be added. In general, this term is proportional to

$$\nabla^2 \frac{\delta H}{\delta b^*(t, \mathbf{k})} \tag{7}$$

and small in the hydrodynamic parameter in comparison with the term  $\omega b$  in Eq. (6). It means that we can ignore nonlinear terms in the dissipation part of the dynamical equation. Thus, to take into account the dissipation terms it is necessary to replace in Eq. (6)  $\omega(k) \rightarrow \omega(k) - i\gamma_0(k)$ , where  $\gamma_0(k) = Dk^2$ .

It is suitable to use for our problem the dynamic diagram technique proposed by Wyld [9] and developed by de Dominicis [10] and Jannsen [11]. Textbook description of this technique can be found in Ref. [12]. The corresponding effective action can be written in the form

$$I = i \int \frac{dt d^3k}{(2\pi)^3} \left\{ \left( p^*(\mathbf{k})[\omega(k) - i\partial_t - i\gamma_0(k)]b(\mathbf{k}) + \lambda \exp(-i2\omega_0 t)p^*(\mathbf{k})b^*(-\mathbf{k}) + \int \frac{d^3q}{(2\pi)^3} V p^*(\mathbf{k})b(\mathbf{q})[2b^*(\mathbf{q} - \mathbf{k}) + b(\mathbf{k} - \mathbf{q})] \right) + \text{c.c.} + T \frac{\gamma_0(k)}{\omega(k)} p^*(\mathbf{k})p(\mathbf{k}) \right\}. \tag{8}$$

Here we have introduced an auxiliary field  $p(t, \mathbf{r})$ , which is conjugated to the wave field  $b(t, \mathbf{r})$ ;  $\lambda \equiv 2aU$  is the pumping field, and  $T$  is the temperature in units of energy. We assumed that the pumping wave is a monochromatic wave with a frequency  $2\omega_0$ . For simplicity we will ignore below the nonzero value of the wave vector of the pumping wave. It is possible if the velocity of the pumping wave is significantly greater than the velocity of excited waves.

The equations of motion (6) with dissipation terms can be obtained as the extremum conditions for the effective action:

$$\frac{\delta I}{\delta p^*(t, \mathbf{k})} = 0, \quad \frac{\delta I}{\delta p(t, \mathbf{k})} = 0.$$

Various averages can be found as

$$\langle f(t, \mathbf{k}) \rangle = \int \mathcal{D}p \mathcal{D}p^* \mathcal{D}b \mathcal{D}b^* f(t, \mathbf{k}) e^{iI}. \tag{9}$$

## 3. THE CORRELATION FUNCTIONS

The quadratic part of the effective action (8) determines the bare correlation functions. There are three types of correlation functions in the Wyld diagram technique. The first  $\langle pb \rangle$  is the Green's function, which is the response function on the external field. The second  $\langle bb \rangle$  is the correlation function. The last average  $\langle pp \rangle$  equals zero. In our system there are normal Green's and correlation functions, which are determined by the term with the coefficient  $\omega - i\gamma_0$ , and the abnormal functions, which are determined by the term with the pumping,  $\lambda = 2aU$ . Let us make Fourier transform over time:

$$b(t, \mathbf{k}) = \int \frac{d\omega}{2\pi} b(\omega, \mathbf{k}) e^{-i\omega t}.$$

Further, for simplicity we introduce the notation

$$\kappa \equiv \{\omega, \mathbf{k}\}, \quad \bar{\kappa} \equiv \{2\omega_0 - \omega, -\mathbf{k}\}, \quad \bar{\omega} = \omega - \omega_0.$$

It is suitable to determine the Green's functions  $\langle bp \rangle$  in the following way:

$$G(\kappa) = \begin{pmatrix} G_1(\kappa) & G_2(\kappa) \\ G_2^*(\bar{\kappa}) & G_1^*(\bar{\kappa}) \end{pmatrix}, \quad (10)$$

where

$$\begin{aligned} \langle b(\kappa) p^*(\kappa_1) \rangle &= (2\pi)^4 \delta(\omega - \omega_1) \delta(\mathbf{k} - \mathbf{k}_1) G_1(\omega, \mathbf{k}), \\ \langle b(\kappa) p(\kappa_1) \rangle &= (2\pi)^4 \delta(\bar{\omega} + \bar{\omega}_1) \delta(\mathbf{k} + \mathbf{k}_1) G_2(\omega, \mathbf{k}). \end{aligned} \quad (11)$$

For the Green's functions  $\langle pb \rangle$  we have

$$\tilde{G}(\kappa) = \begin{pmatrix} G_1^*(\kappa) & G_2(\bar{\kappa}) \\ G_2^*(\kappa) & G_1(\bar{\kappa}) \end{pmatrix}. \quad (12)$$

The bare Green's functions can be found as

$$G_0^{-1}(\kappa) = \begin{pmatrix} ck - \omega - i\gamma_0(k) & \lambda \\ \lambda^* & ck + \omega - 2\omega_0 + i\gamma_0(k) \end{pmatrix}, \quad (13)$$

where  $\gamma_0(k)$  is a bare decrement of the sound wave. It is easy to obtain the following expressions for the bare Green's functions from (13):

$$G_{10}(\kappa) = \Delta^{-1}(\kappa) [ck + \omega - 2\omega_0 + i\gamma_0(k)], \quad G_{20}(\kappa) = -\lambda \Delta^{-1}(\kappa). \quad (14)$$

Here

$$\Delta(\kappa) = (ck - \omega_0)^2 - [\omega - \omega_0 + i\gamma_0(k)]^2 - |\lambda|^2, \quad \Delta(\bar{\kappa}) = \Delta^*(\kappa). \quad (15)$$

The off-diagonal components of the Green's function are essential only for  $\omega \sim \omega_0$  and  $k \sim k_0 \equiv \omega_0/c$ . Far from this region it is possible to use for the Green's function the expression

$$G_1(\kappa) = [ck - \omega - i\gamma_0(k)]^{-1}. \quad (16)$$

The full Green's function can be found as a solution of the Dyson equation in the form

$$G^{-1}(\kappa) = G_0^{-1}(\kappa) - \Sigma(\kappa), \quad (17)$$

where  $\Sigma(\kappa)$  is a self-energy function. The self-energy matrix has the same properties as  $G$ ; i.e., it can be written in the form

$$\Sigma(\kappa) = \begin{pmatrix} \Sigma_1(\kappa) & \Sigma_2(\kappa) \\ \Sigma_2^*(\bar{\kappa}) & \Sigma_1^*(\bar{\kappa}) \end{pmatrix}. \quad (18)$$

The bare value of  $\Sigma(\kappa)$  equals zero.

The correlation function  $F$  has a matrix structure also. It can be determined as

$$F(\kappa) = \begin{pmatrix} F_1(\kappa) & F_2(\kappa) \\ F_2^*(\bar{\kappa}) & F_1^*(\bar{\kappa}) \end{pmatrix}, \quad (19)$$

where

$$\begin{aligned} \langle b(\kappa)b^*(\kappa_1) \rangle &= (2\pi)^4 \delta(\omega - \omega_1) \delta(\mathbf{k} - \mathbf{k}_1) F_1(\omega, \mathbf{k}), \\ \langle b(\kappa)b(\kappa_1) \rangle &= (2\pi)^4 \delta(\bar{\omega} + \bar{\omega}_1) \delta(\mathbf{k} + \mathbf{k}_1) F_2(\omega, \mathbf{k}). \end{aligned}$$

It is easy to see that  $F_1^*(\kappa) = F_1(\kappa)$  and  $F_2(\bar{\kappa}) = F_2(\kappa)$ . Therefore, we can write

$$F(\kappa) = \begin{pmatrix} F_1(\kappa) & F_2(\kappa) \\ F_2^*(\kappa) & F_1(\bar{\kappa}) \end{pmatrix}. \quad (20)$$

The Wyld correlation functions can be calculated as

$$F(\kappa) = G(\kappa)\Phi(\kappa)\tilde{G}(\kappa), \quad (21)$$

where  $\tilde{G}(\kappa)$  is determined by (12), and  $\Phi(\kappa)$  is a force function. Its bare value  $\Phi_0$  is determined by a casual force correlator, i.e.,

$$\Phi_0(\kappa) = \Gamma_0 E, \quad \Gamma_0 = T \frac{\gamma_0(k)}{\omega(k)}, \quad (22)$$

where  $E$  is a unit  $2 \times 2$  matrix. For the bare correlation functions we obtain

$$F_{10}(\kappa) = \Gamma_0 \frac{(ck + \omega - 2\omega_0)^2 + \gamma_0^2(k) + |\lambda|^2}{\Delta(\kappa)\Delta^*(\kappa)}, \quad F_{20}(\kappa) = -\Gamma_0 \frac{2\lambda[ck - \omega_0 + i\gamma_0(k)]}{\Delta(\kappa)\Delta^*(\kappa)}. \quad (23)$$

The force function  $\Phi(\kappa)$  can be written in the form

$$\Phi(\kappa) = \begin{pmatrix} \Phi_1(\kappa) & \Phi_2(\kappa) \\ \Phi_2^*(\kappa) & \Phi_1(\bar{\kappa}) \end{pmatrix}. \quad (24)$$

The force functions  $\Phi(\kappa)$ , by analogy with  $F(\kappa)$ , have the properties  $\Phi_1(\kappa) = \Phi_1^*(\kappa)$  and  $\Phi_2(\kappa) = \Phi_2(\bar{\kappa})$ .

4. SATURATION OF THE EXCITED WAVE

In this section we omit the term proportional to the temperature. In this case the fluctuations of the phase of the parametrically excited wave can be ignored and we can assume that there appears a nonzero value of average  $\langle b \rangle$  if the pumping is over the threshold. The equations for this nonzero average coincide with (6). If we disregard the nonlinear terms on  $b$ , these equations will be linear equations with zero right-hand side:

$$G^{-1} \begin{pmatrix} b(\kappa) \\ b(\bar{\kappa}) \end{pmatrix} = 0. \tag{25}$$

They can have a nonzero solution only if the main determinant of the system  $\Delta(\kappa)$ , which is determined by (15), equals zero:

$$\Delta(\kappa) = (ck - \omega_0)^2 - [\omega - \omega_0 + i\gamma_0(k)]^2 - |\lambda|^2 = 0. \tag{26}$$

This equation can first be satisfied for waves with  $\omega = \omega_0$  and  $k = k_0 = \omega_0/c$ . The threshold value of pumping is  $|\lambda| = \gamma_0(k_0) \equiv \gamma_0$ ; i.e.,

$$|a| = \gamma_0/2U. \tag{27}$$

If  $|\lambda| > \gamma_0$ , the nonzero value of average  $\langle b \rangle$  appears. In order to determine its value, we must consider the nonlinear corrections. In a tree approximation it is necessary to take into account the corrections for the self-energy function, shown in Fig. 1. Solid lines in Fig. 1 correspond to field  $b$ , dashed lines — to field  $p$ , and points — to vertices  $V$ . This diagram for  $k' \simeq k$  gives the contribution to the diagonal part of the self-energy function and determines the nonlinear correction to the decrement  $\gamma$ . The diagram in Fig. 1 for  $k' \simeq -k$  corrects the off-diagonal terms of the self-energy function; it renormalizes the pumping  $\lambda$ .

The Green's function of the diagram in Fig. 1 has frequency near  $2\omega_0$  only if  $k' \simeq k \simeq k_1$  and has frequency near zero for all other cases. Taking into account Eq. (4), it is easy to see that in the first case the correction is greater than that in the second case by a factor of  $\omega_0/\gamma_0$ . In particular, this means that for acoustic waves the nonlinear attenuation is significantly more important than renormalization of pumping. This result agrees with the corresponding conclusion for the surface waves, where the three-wave interactions are allowed [4].

In general, the average of the wave field  $b(t, r)$  has the form

$$\langle b(t, r) \rangle = \int d\Omega B(\theta, \varphi) \exp(-i\omega_0 t + ik_0 \mathbf{e}r), \tag{28}$$

where  $\mathbf{e} \equiv \mathbf{e}(\theta, \varphi)$  is the unit vector in the direction which is determined by the angles  $\theta, \varphi$ , and  $d\Omega \equiv d\theta d\varphi \sin \theta$ . We see that it is possible to disregard the renormalization of the pumping for the sound waves. We will also see that there is no standard pattern formation for sound waves. This means that we can choose a real amplitude  $B$  and a real pumping  $\lambda$ . The correction for the self-energy function in Fig. 1 can be written as



Fig. 1. Tree correction for the self-energy function

$$\begin{aligned}\Sigma(\omega_0, \mathbf{k}) &= 4 \int \frac{d\omega_1 d\mathbf{k}_1}{(2\pi)^4} V^2 F_1(\kappa_1) G_1(\kappa + \kappa_1) \pm \\ &= 4 \int d\theta d\varphi \frac{V^2(\theta, \varphi) B^2(\theta, \varphi) \sin \theta}{\omega(\mathbf{k} + \mathbf{k}_1) - 2\omega_0 - i\gamma(\mathbf{k} + \mathbf{k}_1)}.\end{aligned}\quad (29)$$

In Eq. (29)  $\theta$  is a polar angle between the wave vectors  $\mathbf{k}$  and  $\mathbf{k}_1$ , and  $\varphi$  is the azimuthal angle. Since we use the tree approximation in this section, it is possible to replace

$$\langle b(\kappa) b^*(\kappa_1) \rangle = \langle b(\kappa) \rangle \langle b^*(\kappa_1) \rangle.$$

It is easy to see that the integral in (29) is determined by the small region at the angle  $\theta$ ,  $\Delta\theta \simeq 4\sqrt{\gamma_0/\omega_0}$ . In this region it is possible to replace  $V(\theta, \varphi)$  and  $B(\theta, \varphi)$  by its values for  $\theta = 0$  and use instead of  $\sin \theta$  the approximate expression  $\sin \theta \simeq \theta$ . As a result, we obtain  $\omega(\mathbf{k} + \mathbf{k}_1) \simeq 2\omega_0(1 - \theta^2/8)$ . The real and the imaginary parts of  $\Sigma$  are of the same order of magnitude. Since  $\omega_0 \gg \gamma_0$ , it is possible to ignore the real part of  $\Sigma$ , which gives a small correction for the sound velocity. The imaginary part of  $\Sigma$  gives the correction for the decrement  $\gamma$ :

$$\gamma = \gamma_0 + \text{Im} \Sigma. \quad (30)$$

For the imaginary part of  $\Sigma$  we have

$$\begin{aligned}\text{Im} \Sigma(\omega_0, k_0 \mathbf{e}) &\equiv \mu n(\mathbf{e}), \quad n(\mathbf{e}) = B^2(\mathbf{e}), \\ \mu &= 4V^2 \int d\theta d\varphi \frac{\gamma_0(2k_0) \sin \theta}{[\omega(\mathbf{k} + \mathbf{k}_1) - 2\omega_0]^2 + \gamma_0^2(2k_0)},\end{aligned}\quad (31)$$

where  $V \equiv V(\theta = 0)$ . The equilibrium value of the amplitude of the excited wave is defined as

$$\lambda \equiv \gamma_0(1 + \epsilon) = \gamma_0 + \mu n, \quad n = \gamma_0 \epsilon / \mu. \quad (32)$$

Therefore, the equilibrium density  $n$  of the parametrically excited wave propagating in a given direction  $\mathbf{e}$  is proportional to  $\epsilon$ .

In further calculations it is necessary to make some assumptions about the shape of parametrically excited wave. If we ignore the nonzero value of the wave vector of the pumping wave and if the system is isotropic (in particular, if the vertex  $U$  of the interaction of the pumping wave with the excited waves depends only slightly on the angles), the excited wave will be a spherical wave (three-dimensional):

$$\langle b(t, \mathbf{r}) \rangle_3 = B \int d\Omega \exp(-i\omega_0 t + ik_0 \mathbf{e} \mathbf{r}). \quad (33)$$

In this case the coefficient  $\mu$  is

$$\mu_3 = 8\pi^2 V^2 \omega_0^{-1}. \quad (34)$$

The total density of the excited wave is

$$N_3 = 4\pi B^2 = \frac{2}{\pi} \frac{\gamma_0 \omega_0}{4V^2} \epsilon. \quad (35)$$

It is interesting to compare this result with the corresponding answer for spin waves [2]. Saturation of the amplitude of the excited spin wave occurs due to the renormalization of

pumping by the four-wave interaction (dephasing mechanism). The corresponding result for the density of the wave is  $n \propto \sqrt{\epsilon}$ . Estimate for the proportionality coefficient in this equation coincides with the estimate for the coefficient in (34) but it turns out that the coefficient for the four-wave interaction is greater numerically. Besides near the threshold  $\epsilon \ll \sqrt{\epsilon}$ , so the nonlinear attenuation due to the three-wave interaction is more important than the renormalization of pumping by the four-wave interaction.

If the system has axial symmetry or if the pumping wave is a standing wave, as is the case in Ref. [5], it is possible that the excited wave will be a cylindrical wave:

$$\langle b(t, \mathbf{r}) \rangle_2 = B \int d\varphi \exp[-i\omega_0 t + ik_0(x \cos \varphi + y \sin \varphi)]. \quad (36)$$

In this case the coefficient  $\mu$  and the total density of the wave will be

$$\mu_2 = 2^{3/2} \frac{\pi V^2}{\sqrt{\omega_0 \gamma_0}}, \quad N_2 = 2\pi B^2 = 2^{3/2} \sqrt{\frac{\gamma_0}{\omega_0}} \frac{\gamma_0 \omega_0}{4V^2} \epsilon. \quad (37)$$

A further decrease of the symmetry can render an excited wave flat. In this case the corresponding equations will be

$$\langle b(t, \mathbf{r}) \rangle_1 = 2B \exp(-i\omega_0 t) \cos(k_0 x), \quad \mu_1 = 4 \frac{V^2}{\gamma_0}, \quad N_1 = B^2 = \frac{\gamma_0}{\omega_0} \frac{\gamma_0 \omega_0}{4V^2} \epsilon. \quad (38)$$

For the last two cases the restriction of the sound-wave amplitude by nonlinear attenuation is stronger than the corresponding saturation due to the dephasing mechanism by a factor of  $\sqrt{\gamma_0/\omega_0}$  for a cylindrical wave and by a factor of  $\gamma_0/\omega_0$  for a flat wave.

The total intensity of parametrically excited sound wave is maximal for a spherical wave and minimal for a flat wave. This situation for sound waves is quite different from the situation for spin waves, where the integral intensity of parametrically excited wave depends only slightly on its shape. In general, it is natural to expect that a nonlinear system will try to have maximal full intensity and corresponding dissipation. This means that it is possible to expect transitions from a less symmetric shape to a more symmetric shape of the sound wave (for example, flat  $\rightarrow$  cylindrical  $\rightarrow$  spherical) as the intensity of the pumping wave increases. This means that it is necessary to expect the appearance of a sound wave with the maximum possible symmetry near the threshold.

Sound waves interact essentially only if the angle between their wave vectors is smaller than  $\Delta\theta \simeq 4\sqrt{\gamma_0/\omega_0}$ . This peculiar property of the interaction destroys the long-range order at an angle between the sound waves and leads to the absence of an ordinary pattern formation. Specific patterns which must appear over the threshold of excitation of sound waves have approximately equal intensities of the waves propagating in the range from  $-\Delta\theta$  to  $\Delta\theta$ . In an anisotropic system the shape of parametrically excited wave is determined mainly by the shape of the pumping wave, by the properties of the interaction vertex between the pumping wave and the excited waves, and by the boundary conditions.

## 5. THERMAL BROADENING

Let us consider the influence of thermal fluctuations on the spectrum of a parametrically generated sound wave. It is necessary to take into account the diagram in Fig. 2, which

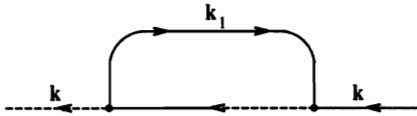


Fig. 2. One-loop correction for the normal self-energy function

contributes to the self-energy function  $\Sigma_1(k)$ . Analytical expression for this diagram is determined by (29), where now the function  $F_1$  is irreducible. The matrix structure of the correlation functions is essential only for the frequencies near  $\omega_0$ . For the diagram in Fig. 2 it is therefore necessary to take into account the nondiagonality of the function  $F_1$  and use for it the expression (23). The Green's function  $G$  has the frequency  $\omega \sim 2\omega_0$ , so we can use for it the expression (16). Equation (29) now can be rewritten as

$$\Sigma_1(\omega, \mathbf{k}) = 4V^2 \int \frac{d\omega_1 d\mathbf{k}_1}{\Omega(2\pi)^4} \Gamma_0(k_1) \frac{(ck_1 + \omega_1 - 2\omega_0)^2 + \gamma^2 + \lambda^2}{|(\omega_1 - i\gamma)^2 - (ck_1 - \omega_0)^2 + \lambda^2|^2} \int d\Omega G_1(\kappa). \quad (39)$$

The last integration in Eq. (39) must be made over all angles. For a flat wave it is absent, for a cylindrical wave it is an integral over an angle  $\theta$ , and for a spherical wave it is an integral over  $d\Omega = d\theta d\varphi \sin \theta$ . In Eq. (39) the first integral is real and the imaginary part of the second integral is determined by (31). The integral from the correlation function  $F$  over  $\mathbf{k}_1$  determines the spectral density of excited sound waves. This density can be determined from the equation

$$n = \int d\omega n(\omega) = \frac{1}{\Omega} \int \frac{d\omega d\mathbf{k}}{(2\pi)^4} F_1(\omega, \mathbf{k}). \quad (40)$$

Here  $n$  and  $n(\omega)$  are the integral and spectral densities of the sound waves, which propagate in a given direction. The factor  $\Omega$  in (39) and (40) depends on the shape of the wave. For a spherical wave  $\Omega = 4\pi$ , for a cylindrical wave  $\Omega = 2\pi$  and for a flat wave  $\Omega = 1$ . The spectral density of a wave is introduced in such a way that the total density  $N$  of the sound wave is

$$N = \Omega n.$$

The first integral in Eq. (39) contains the function  $F$ , which is singular on  $\omega_1, k_1$ , and smooth function  $\int d\Omega G$ . It is possible to write instead of the second integral the expression (31) and consider it as a constant factor. Thus the renormalized attenuation rate of the sound wave is

$$\gamma = \gamma_0 + \text{Im} \Sigma, \quad \text{Im} \Sigma = \mu n. \quad (41)$$

Here  $n$  is the total spectral density of the excited sound waves, which propagate in a given direction, obtained with allowance for thermal broadening. Calculating the first integral in (39), we obtain the equation for the damping rate  $\gamma$ . We can consider this equation as self-consistent equation for  $\gamma$ , which means that we have summed the set of diagrams in Fig. 2:

$$\gamma = \gamma_0 + K\Gamma_0/\nu, \quad \nu \equiv \sqrt{\gamma^2 - \lambda^2}. \quad (42)$$

For simplicity it is useful to choose real  $\lambda$ . The coefficient  $K$  is

$$K = \mu \frac{k_0^2(\gamma^2 + \lambda^2)}{16\pi^2 c \gamma}. \quad (43)$$

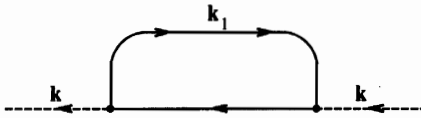


Fig. 3. One-loop correction for the normal force function

Now the value of  $\gamma$  must be found from Eq. (42). We see that  $\gamma > 0$  for all values of the pumping  $\lambda$ . The width of the distribution  $n(\omega)$  is determined by the position of the singularity nearest to the real axis in the integral  $\int d\omega_1 F_1$ . For  $\lambda > \gamma_0$  this width is of the order of  $\nu$ . If  $\lambda \gg \gamma_0$ , the value of  $\gamma$  can be determined from the equation

$$\gamma \simeq \frac{K\Gamma_0}{\sqrt{\gamma^2 - \lambda^2}}. \tag{44}$$

We see that thermal width of the spectrum leads to zero if  $\lambda \rightarrow \infty$ . It is easy to determine the spectral distribution  $n(\omega)$ . We have

$$n(\omega) = \Gamma_0 \frac{k_0^2(\gamma^2 + \lambda^2)}{(2\pi)^3 c} J, \quad J = \int \frac{dk}{|c^2 k^2 + (\gamma + i\omega)^2 - \lambda^2|^2}. \tag{45}$$

The poles of the integrated function are  $k = \pm ia_{\pm}$ , where  $a_{\pm} = \sqrt{(\gamma \pm i\omega)^2 - \lambda^2}$ . If  $\omega < \nu^2/2\gamma$ , than these poles lie near the real axis at a distance of the order of  $\nu$ . If  $\omega > \nu^2/2\gamma$ , the corresponding distance is about  $\gamma\omega/\sqrt{\gamma^2 + \lambda^2}$ . The main part of the integral is produced from the first region. Calculating this part, we obtain

$$J = \frac{\pi}{2\nu^3 f(\bar{\omega})}, \quad f(x) = \frac{r^2}{\sqrt{2}} \sqrt{r^2 + 1 - x^2\nu^{-2}}, \quad r^2 = \sqrt{(1 - x^2\nu^{-2})^2 + 4\gamma^2 x^2\nu^{-4}}. \tag{46}$$

For spectral distribution of the sound waves we have

$$n(\omega) = \frac{k_0^2}{(2\pi)^3 c} \frac{\pi(\gamma^2 + \lambda^2)}{2\nu^3} \frac{\Gamma_0}{f(\bar{\omega})}. \tag{47}$$

Let us compare Eqs. (41) and Eq. (32), which was obtained for the distribution of zero width. Let  $(\Delta\omega)_T$  be the thermal width of the spectrum. For  $\lambda - \gamma_0 \gg (\Delta\omega)_T$  we have  $\gamma - \lambda \ll \gamma_0$ . Therefore, integrating the distribution  $n(\omega)$  over  $\omega$ , we obtain the integral intensity of excited sound waves, which coincides with the previous result (32) for the intensity.

In a one-loop approximation it is necessary to take into account the correction to the force function, which can be represented by the diagram in Fig. 3. The analytical expression for this correction is

$$(\Phi_1(\kappa))_1 \sim \frac{V^2}{\Omega} \int \frac{d\omega_1 d\mathbf{k}_1}{(2\pi)^4} F_1(\kappa_1) F_1(\kappa + \kappa_1). \tag{48}$$

Here the first function  $F_1$  has a frequency near  $\omega_0$  and the second function  $F_1$  has a frequency near  $2\omega_0$ . We can calculate (48) as an analogous expression for  $\Sigma_1$ . For the second function  $F_1$  we can use the expression

$$F_1(\kappa + \kappa_1) = \frac{2T\gamma_0}{c\omega \left\{ [\omega(|\mathbf{k} + \mathbf{k}_1|) - \omega - \omega_1]^2 + \gamma_0^2(2k_0) \right\}}. \tag{49}$$

We can then write Eq. (48) in the form

$$(\Phi_1(\kappa))_1 \sim \frac{V^2}{\Omega} \int \frac{d\omega_1 d\mathbf{k}_1}{(2\pi)^4} F_1(\kappa_1) \int d\Omega F(\kappa + \kappa_1). \tag{50}$$

The first integral was found in (39); for the second integral we have

$$\int d\Omega F(\kappa + \kappa_1) = \frac{T\mu}{\omega_0 V^2}. \tag{51}$$

Thus, for the force function we have

$$(\Phi_1)_1 \sim V^2 \frac{Tn}{\omega_0 \sqrt{\omega_0 \gamma_0}} \tag{52}$$

and

$$\frac{(\Phi_1)_1}{\Phi_{10}} \sim \frac{\mu n T}{\omega_0} \frac{\omega_0}{T \gamma_0} \propto \epsilon. \tag{53}$$

This correction is small near the excitation threshold. Therefore, in a one-loop approximation it is possible to consider only the broadening of parametrically excited waves due to thermal fluctuations. Thermal width of the spectrum is very small, and its dependence on pumping does not agree with the experiment. This means that it is necessary to use a two-loop approximation in order to describe the experimentally observed broadening of the spectrum.

### 6. TWO-LOOP CORRECTIONS

To study the broadening of excited sound waves due to their scattering we must take into account the two-loop corrections for the mass operators: the self-energy function  $\Sigma$  and the force function  $\Phi$ . These corrections for  $\Sigma_1$  and  $\Sigma_2$  can be represented by the diagrams in Fig. 4.

Their analytical representation is

$$\begin{aligned} \Sigma_1(\kappa) &= 8V^4 \int \frac{d^4 \kappa_1 d^4 \kappa_2}{(2\pi)^8} [G_1^*(\kappa_1) F_1(\kappa_2) F_1(\kappa_1 + \kappa - \kappa_2) G(\kappa + \kappa_1) G^*(\kappa + \kappa_1) + \\ &\quad + 2G_1(\kappa_1) F_2(\kappa_2) F_2^*(\kappa_1 + \kappa_2 - \kappa) G(\kappa_1 + \kappa_2) G(\kappa - \kappa_2)], \\ \Sigma_2(\kappa) &= 8V^4 \int \frac{d^4 \kappa_1 d^4 \kappa_2}{(2\pi)^8} [G_2^*(\kappa_1) F_2(\kappa_2) F_2(\kappa_1 + \kappa - \kappa_2) G(\kappa + \kappa_1) G(-\kappa - \kappa_1) + \\ &\quad + 2G_2(\kappa_1) F_1(\kappa_2) F_1(\kappa_1 + \kappa_2 - \kappa) G(\kappa_1 + \kappa_2) G^*(\kappa_2 - \kappa)]. \end{aligned} \tag{54}$$

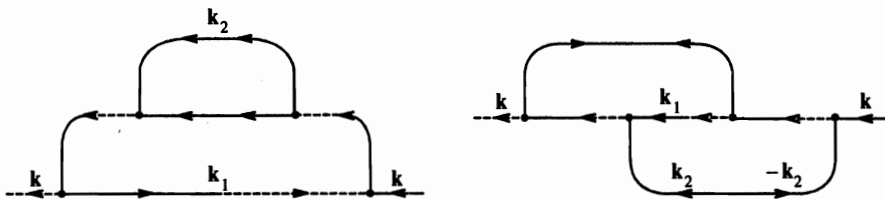


Fig. 4. Two-loop corrections for the normal self-energy function

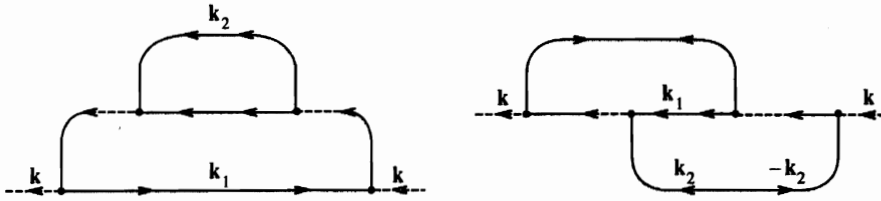


Fig. 5. Two-loop corrections for the normal force function

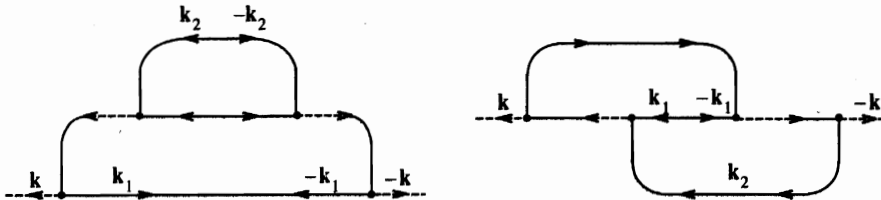


Fig. 6. Two-loop corrections for the abnormal force function

The corresponding diagrams for  $\Phi_1$  and  $\Phi_2$  are presented in Figs. 5 and 6. Analytically, we have

$$\begin{aligned} \Phi_1(\kappa) = 8V^4 \int \frac{d^4 \kappa_1 d^4 \kappa_2}{(2\pi)^8} [F_1(\kappa_1)F_1(\kappa_2)F_1(\kappa_1 + \kappa - \kappa_2)G(\kappa + \kappa_1)G^*(\kappa + \kappa_1) + \\ + 2F_1(\kappa_1)F_2(\kappa_2)F_2^*(\kappa_1 + \kappa_2 - \kappa)G(\kappa_1 + \kappa_2)G^*(\kappa - \kappa_2)], \end{aligned} \tag{55}$$

$$\begin{aligned} \Phi_2(\kappa) = 8V^4 \int \frac{d^4 \kappa_1 d^4 \kappa_2}{(2\pi)^8} [F_2^*(\kappa_1)F_2(\kappa_2)F_2(\kappa_1 + \kappa - \kappa_2)G(\kappa + \kappa_1)G(-\kappa - \kappa_1) + \\ + 2F_2(\kappa_1)F_1(\kappa_2)F_1^*(\kappa_1 + \kappa_2 - \kappa)G(\kappa_1 + \kappa_2)G(\kappa_2 - \kappa)]. \end{aligned}$$

It is easy to test that the expressions for  $\Phi_1(\kappa)$  and  $\Phi_2(\kappa)$  satisfy the properties  $\Phi_1(\kappa) = \Phi_1^*(\bar{\kappa})$  and  $\Phi_2(\kappa) = \Phi_2(\bar{\kappa})$ .

The corrections for the Green's functions and for the correlation functions, represented by the second terms in Eqs. (54) and (55), can be disregarded. In fact, it is necessary to take into account only the diagrams, which contain the correlation functions  $F(\omega)$  with  $\omega \sim \omega_0$  and the Green's functions  $G(\omega)$  with  $\omega \sim \omega_0$  or  $\omega \sim 2\omega_0$ . It is impossible to satisfy these conditions for the corrections mentioned above. The first correction term for  $\Phi_2$  ( $\Sigma_2$ ) will then be significantly smaller than the corresponding term for  $\Phi_1$  ( $\Sigma_1$ ), because the distance between the poles of the corresponding Green's functions is of the order of  $2\omega_0$  in the first case and of the order of  $8\gamma_0$  in the second case. This means that we can rewrite Eqs. (54) and (55) in the form

$$\Sigma_1(\kappa) = 8V^4 \int \frac{d^4 \kappa_1 d^4 \kappa_2}{(2\pi)^8} G_1^*(\kappa_1)F_1(\kappa_2)F_1(\kappa_1 + \kappa - \kappa_2)G(\kappa + \kappa_1)G^*(\kappa + \kappa_1), \tag{56}$$

$$\Sigma_2(\kappa) \simeq 0$$

and

$$\Phi_1(\kappa) = 8V^4 \int \frac{d^4 \kappa_1 d^4 \kappa_2}{(2\pi)^8} F_1(\kappa_1) F_1(\kappa_2) F_1(\kappa_1 + \kappa - \kappa_2) G(\kappa + \kappa_1) G^*(\kappa + \kappa_1), \tag{57}$$

$$\Phi_2(\kappa) \simeq 0.$$

Here and below the functions  $G(\kappa)$  have the frequencies  $\omega \sim 2\omega_0$ ; therefore, we can use for them expression (16).

Equations (56) and (57) mean that in a two-loop approximation we have a situation similar to a one-loop approximation. It turns out that the corrections for the abnormal self-energy and for the abnormal force functions are significantly smaller than the corresponding corrections for the normal functions. The corrections for the self-energy functions can be taken into account if we replace

$$\gamma_0(\kappa) \rightarrow \gamma(\kappa) = \gamma_0(\kappa) + \mu n + (\text{Im } \Sigma_1(\kappa))_2 \tag{58}$$

and if we use Eqs. (14) and (15). Here we took into account the tree correction for the self-energy function, shown in Fig. 1. Analogously, the corrections for the correlation functions can be taken into account if we replace

$$\Gamma_0(\kappa) \rightarrow \Gamma(\kappa) = \Gamma_0(\kappa) + \Phi_1(\kappa) \tag{59}$$

and if we use Eq. (23). In the last equation it is possible to ignore both the first term and the one-loop correction for the force function  $\Phi_1$ , because they are very small.

Thus, we obtain the following equation for the two-loop correction for the self-energy functions:

$$(\Delta\gamma)_2 = -8V^4 \int \frac{d^4 \kappa_1 d^4 \kappa_2}{(2\pi)^8} \frac{(ck_1 + \omega_1 - 2\omega_0)^2 + \gamma^2 - \lambda^2}{\Delta(\kappa_1)\Delta^*(\kappa_1)} \times \\ \times \gamma(\kappa_1) F_1(\kappa_2) F_1(\kappa_1 + \kappa - \kappa_2) G(\kappa + \kappa_1) G^*(\kappa + \kappa_1). \tag{60}$$

The corresponding equation for the force function has the form

$$\Gamma(\kappa) = 8V^4 \int \frac{d^4 \kappa_1 d^4 \kappa_2}{(2\pi)^8} F_1(\kappa_1) F_1(\kappa_2) F_1(\kappa_1 + \kappa - \kappa_2) G(\kappa + \kappa_1) G^*(\kappa + \kappa_1). \tag{61}$$

First, let us consider the case in which the excited sound wave is spherical. It is easy to integrate in (60) and (61) over the angles  $\vartheta(\mathbf{k}_1, \mathbf{k})$  and  $\varphi(\mathbf{k}_1, \mathbf{k})$ . The only factor in these expressions, which depends on the angle  $\vartheta$ , is  $G(\kappa + \kappa_1)G^*(\kappa + \kappa_1)$ . For the integral we have

$$\int \frac{d\vartheta(\mathbf{k}_1, \mathbf{k}) d\varphi(\mathbf{k}_1, \mathbf{k}) \sin \vartheta}{[\omega(\mathbf{k} + \mathbf{k}_1) - \omega - \omega_1]^2 + 16\gamma_0^2} = \frac{\pi^2}{2\omega_0\gamma_0}. \tag{62}$$

Note that it is proportional to  $\gamma_0^{-1}$  and therefore this expression is significantly greater than the analogous term for the direct fourth vertex. This statement is true independently of the shape of the excited sound wave. This means that broadening of the spectrum of parametrically excited acoustic wave is determined by the three-wave interaction.

Substituting expression (62) in (60) and (61), we obtain the system of equations

$$\begin{aligned} \gamma(\kappa) &= \gamma_0 + \mu n - C \int \frac{d\omega_1 dk_1 d\omega_2 dk_2 d\theta \sin \theta}{(2\pi)^8} \gamma(k_1) \times \\ &\times \frac{(ck_1 + \omega_1 - 2\omega_0)^2 + \gamma^2 - \lambda^2}{\Delta(\kappa_1)\Delta^*(\kappa_1)} F_1(\kappa_2) F_1(\kappa_1 + \kappa - \kappa_2), \\ \Gamma(\kappa) &= C \int \frac{d\omega_1 dk_1 d\omega_2 dk_2 d\theta \sin \theta}{(2\pi)^8} F_1(\kappa_1) F_1(\kappa_2) F_1(\kappa_1 + \kappa - \kappa_2), \end{aligned} \tag{63}$$

where  $\theta \equiv \theta(\mathbf{k}_1 + \mathbf{k}, \mathbf{k}_2)$ ,  $C = \mu_3 V^2 k_0^4 / 2\gamma_0$ .

As we will see, the two-loop correction for the damping rate  $\gamma$  is not very important. So first let us consider the correction for the force function. It is necessary to use the integrals over  $k_1, k_2$ , and  $\theta$ . Experiment shows that broadening of parametrically excited waves is significantly smaller than  $\gamma \sim \lambda$ . Therefore, we can write

$$\gamma^2(k) - \lambda^2 \equiv \nu^2, \quad \nu \ll \lambda, \quad \Delta(k) = (ck - \omega_0)^2 - \bar{\omega}^2 + \nu^2 - 2i\gamma\bar{\omega}. \tag{64}$$

The characteristic value of  $ck - \omega_0$  is of the order of  $\nu$  and the characteristic value of  $\bar{\omega}$  is of the order of  $\nu^2/2\gamma \ll \nu$ . It is easy to see that the dependence of  $\Gamma(\omega, \mathbf{k})$  on the wave vector  $\mathbf{k}$  is smooth, while its dependence on the frequency  $\omega$  is singular. Therefore, integrating in (63) over  $k_1, k_2$ , and  $\theta$ , we can assume  $\Gamma$  to be a constant, and the corresponding integrals are determined by the poles of  $\Delta(k)\Delta^*(k)$ . The integral over the angle  $d\Omega = d\theta d\phi \sin \theta$  is

$$\int d\Omega F_1(\mathbf{k}_1 + \mathbf{k} - \mathbf{k}_2) = \frac{\pi^2(\gamma^2 + \lambda^2)}{2\omega_0\nu^3} \frac{\Gamma(\omega_1 + \omega - \omega_2)}{f(\zeta)}, \quad \zeta = \omega_1 + \omega - \omega_2 - \omega_0, \tag{65}$$

where  $f(\zeta)$  and  $r$  are determined by (46). For  $\zeta \sim \nu^2/2\gamma$  the function  $f$  can be written as

$$f(\zeta) = \frac{1}{\sqrt{2}} \sqrt{1 + (2\gamma\zeta\nu^{-2})^2} \sqrt{\sqrt{1 + (2\gamma\zeta\nu^{-2})^2} + 1}. \tag{66}$$

It is easy to see that  $f(\zeta)$  is an even function and that  $f(0) = 1$ .

The integral over  $k_1$  gives

$$\int dk_1 F_1(\mathbf{k}) = \frac{\pi(\gamma^2 + \lambda^2)}{2c\nu^3} \frac{\Gamma(\omega_1)}{f(\bar{\omega}_1)}. \tag{67}$$

Thus we obtain the following equation for  $n(\bar{\omega})$ :

$$f(\bar{\omega})n(\omega) = C_3 \int d\omega_1 d\omega_2 n(\omega_1)n(\omega_2)n(\omega_1 + \omega - \omega_2), \quad C_3 = \frac{\mu_3^2(\gamma^2 + \lambda^2)}{8\gamma_0\nu^3}, \tag{68}$$

where  $\mu_3$  is determined by (34).

Analogous equation was obtained for the distribution of parametrically excited spin waves [3]. It is easy to solve this equation for  $f(x) = 1 + (x/\eta)^2$ . In this case the solution is

$$n(\omega) = \left( \sqrt{2C_3\eta} \operatorname{ch}(\pi\bar{\omega}/2\eta) \right)^{-1}$$

General consideration shows that for our functions  $f(x)$ , which have no singularities in the close vicinity of the real axes, the solution of Eq. (68) has a symmetrical form with the center at  $\bar{\omega} = 0$  and exponential frequency asymptotics. The characteristic width of the distribution

can be estimated in a following way. Since  $n = \int d\omega n(\omega) \simeq \sqrt{2/C_3}$  and using the equation for equilibrium density of the sound wave (32), we obtain

$$\mu_3 n = \epsilon \gamma_0 \simeq \sqrt{\frac{16\gamma_0 \nu^3}{\gamma^2 + \lambda^2}}. \tag{69}$$

Numerical coefficient in this equation cannot be found analytically; it is of the order of unity. Thus,

$$\nu \simeq \left( \frac{\gamma_0 \epsilon^2}{8} \frac{\gamma^2 + \lambda^2}{2} \right)^{1/3}. \tag{70}$$

We obtain

$$(\Delta\omega)_3 \simeq \frac{1}{4\pi\gamma} \left( \gamma_0 \epsilon^2 \frac{\gamma^2 + \lambda^2}{2} \right)^{2/3}. \tag{71}$$

Analogously, it is possible to obtain the corresponding equations for the excited cylindrical sound wave. The equation for  $n$  is

$$f(\bar{\omega})n(\omega) = C_2 \int d\omega_1 d\omega_2 n(\omega_1)n(\omega_2)n(\omega_1 + \omega - \omega_2)\tilde{f}(\zeta), \tag{72}$$

$$C_2 = \frac{\mu_2^2(\gamma^2 + \lambda^2)}{16\sqrt{\gamma_0\nu^7}}, \quad \tilde{f}(\zeta) = \sqrt{\frac{1}{r} + \frac{\gamma|\zeta|}{\nu^2 f(\zeta)}},$$

where  $\mu_2$  is determined by (37) and  $r$  is determined by (46). Equation (72) has the same asymptotic form as the corresponding Eq. (68) for a spherical wave. This means that the asymptotic properties of the solution of this equation are the same as for Eq. (68). By analogy with Eqs. (69)–(71), we can obtain for an excited cylindrical sound wave

$$\mu_2 n = \epsilon \gamma_0 \simeq 4(\gamma_0 \nu^7)^{1/4} \sqrt{\frac{2}{\gamma^2 + \lambda^2}}, \quad (\Delta\omega)_2 \simeq \frac{\nu^2}{\pi\gamma} \simeq \frac{(\gamma_0^6 \epsilon^8)^{1/7}}{4\pi\gamma} \left( \frac{\gamma^2 + \lambda^2}{2} \right)^{4/7}. \tag{73}$$

Let us consider the one-dimensional case of a flat sound wave. In this case the dependence of  $\Gamma$  on  $k$  is not smooth. We can obtain the following equation for  $n(\omega, k)$ :

$$\bar{f}(\omega, k)n(\omega, k) = C_1 \int dk_1 d\omega_1 dk_2 d\omega_2 n(\omega_1, k_1)n(\omega_2, k_2)n(\omega_1 + \omega - \omega_2, k_1 + k - k_2),$$

$$\bar{f}(\omega, k)n(\omega, k) = \left[ 1 + \left( \frac{ck - \omega_0}{\nu} \right)^2 \right]^2 + \left( \frac{2\gamma\bar{\omega}}{\nu^2} \right)^2, \quad C_1 = \frac{\mu_1^2}{32} \frac{\gamma^2 + \lambda^2}{\nu^4}, \tag{74}$$

where  $\mu_1$  is determined by (36). Equation (74) means that

$$\mu_1 n = \epsilon \gamma_0 \simeq 8\nu^2 \sqrt{\frac{1}{\gamma^2 + \lambda^2}}. \tag{75}$$

For the width of a sound spectrum we have

$$(\Delta\omega)_1 \simeq \frac{\gamma_0\epsilon}{8\pi\gamma} \sqrt{\gamma^2 + \lambda^2}. \tag{76}$$

Note that numerical coefficients in expressions (71), (73), and (76) are not correct; these equations determine only estimates for the corresponding widths. It is necessary to solve the corresponding nonlinear equations numerically in order to determine accurate values of the coefficients.

Let us now estimate the two-loop correction for the self-energy function. It is easy to obtain from the first equation in (63):

$$\frac{(\Delta\gamma)_2}{(\Delta\gamma)_1} \sim \frac{1}{16} \epsilon^{1/7}. \tag{77}$$

We see that the two-loop correction is small numerically and that it does not change the general picture essentially. This result is logical, because the conservation laws allow us to obtain a not small one-loop correction for the self-energy function. It turns out that the corresponding two-loop correction is not essential. For the force function the one-loop correction is small. It is therefore necessary to take into account the two-loop corrections.

### 7. COMPARISON WITH THE EXPERIMENT

Let us compare the theory with the experiment [5,6]. Experimental studies [5,6] were performed for parametric generation of a second-sound wave by a first-sound wave in liquid helium near the superfluid transition temperature. The canonical variables for this system were found by Pokrovskii and Khalatnikov [8], who calculated the triple vertex  $U$  of the first- and second-sound interaction (the correct vertex is greater than that found by Pokrovskii and Khalatnikov by a factor of 2, in agreement with the result of Lebedev [13]). The correct expression for this vertex is

$$U = \frac{1}{c_1} \sqrt{\frac{\omega_1^3}{32\rho}} \left[ \frac{1}{\rho} \frac{P_{\sigma\sigma}}{T_\sigma} - \frac{\rho}{\rho_s} \left( \frac{\partial \rho_s}{\partial \rho} \right)_\sigma \right]. \tag{78}$$

Here  $\rho$  and  $\rho_s$  are the total and the superfluid density of liquid helium,  $P$  and  $T$  are the pressure and temperature,  $\omega_1$  is the frequency of the first sound,  $c_1$  its velocity,  $\sigma = S/\rho$ ;  $T_\sigma = (\partial T/\partial \sigma)_\rho$ , etc. For experimental conditions of Refs. [5] and [6], it is possible to ignore the weak dependence of this vertex on the angle between the wave vectors, which is small as  $\rho_s/\rho$ . Expression (78) can be rewritten in the variables  $P, T$  in the following way:

$$U = \frac{1}{c_1} \sqrt{\frac{\omega_1^3}{32\rho}} (U_1 + U_2), \tag{79}$$

where

$$U_1 = -\frac{\rho}{J\phi} \left( \frac{C_P}{T} \frac{\partial \phi}{\partial P} + \frac{\beta_P}{\rho} \frac{\partial \phi}{\partial T} \right), \quad U_2 = \rho^{-1} \left( \frac{\partial \psi}{\partial T} + \frac{\beta_P}{\kappa_T} \frac{\partial \psi}{\partial P} \right). \tag{80}$$

Here we introduce the notation

$$\begin{aligned} \phi &= \frac{\rho_s}{\rho}, \quad \psi = \frac{\rho\beta_P}{J}, \quad J = \frac{\rho\kappa_T C_P}{T} - \beta_P^2, \quad \kappa_T = \frac{1}{\rho} \left( \frac{\partial \rho}{\partial P} \right)_T, \\ C_P &= T \left( \frac{\partial \sigma}{\partial T} \right)_P, \quad \beta_P = -\rho \left( \frac{\partial \sigma}{\partial P} \right)_T = -\frac{1}{\rho} \left( \frac{\partial \rho}{\partial T} \right)_P. \end{aligned} \tag{81}$$

Here  $\omega_2$  and  $c_2$  are the frequency and the velocity of the second sound. These equations permit us to use the results of Ref. [14] to calculate this vertex.

Using the Pokrovskii-Khalatnikov equations for the canonical variables, we obtain the following expression for the triple vertex of the second-sound interaction:

$$V(\theta) = \sqrt{\frac{\omega_2}{16\rho T_\sigma}} \left\{ \frac{T_{\sigma\sigma}}{T_\sigma} + \frac{1}{\rho_s} \left( \frac{\partial \rho_s}{\partial \sigma} \right)_\rho [\cos(2\theta) - 2 \cos \theta] \right\}, \tag{82}$$

where  $\theta$  is the angle between the wave vectors of the second-sound waves. This vertex can be written in the variables  $P, T$  as

$$V(\theta) = \sqrt{\frac{\omega_2^3}{16\rho}} X, \quad X = \sqrt{\chi} \left\{ \frac{1}{\chi} \hat{D}(\chi) + \frac{1}{\phi} \hat{D}(\phi) [\cos(2\theta) - 2 \cos \theta] \right\}, \tag{83}$$

where

$$\chi = \frac{\rho\kappa_T}{J}, \quad \hat{D} = \frac{\partial}{\partial T} + \frac{\beta_P}{\kappa_T} \frac{\partial}{\partial P}.$$

It is possible to compare the experimental results with theory for three parameters: the threshold of the second sound excitation, the equilibrium intensity of the second-sound over the threshold, and the form of the spectrum of the excited waves. The ratio of the velocities of the pumping first-sound wave and the excited second sound waves was about  $10^{-2}$  in [5]. The pumping wave was a standing wave. These facts lead to a generation of cylindrical (or perhaps flat) but not a spherical second-sound wave. It is possible to see that an accurate comparison of the data on the excitation threshold with Eqs. (27), (79), and (80) gives a good agreement, significantly better than that in Ref. [5]. It is necessary to point out, however, that for the experiment [5] Eq. (27) must be modified. A special geometry of the experimental cell and pumping by a standing wave lead to the following modified equation for the excitation threshold:

$$|a| = \gamma_0 / \sqrt{2U}.$$

A correlation of the second-sound waves for intermediate angles between the wave vectors was not observed experimentally. This result agrees with our statement about the absence of long-range order on the angle for parametrically generated sound waves.

The thermal width near the threshold can be easily estimated for a given experiment [5]. In fact,

$$(\Delta\omega)_T = \frac{K\Gamma_0}{\sqrt{\gamma^2 - \lambda^2}} \sim \mu \frac{\omega_0\gamma_0 T}{4\pi^2 c_2^3} \sim \gamma_0 \frac{\omega_0\gamma_0 T}{4\pi^2 c_2^3 n}. \tag{84}$$

The value of  $n$  can be found from the second-sound intensity  $\tilde{I}$ :

$$\tilde{I} = c_2\omega_2 n,$$

and we have

$$(\Delta\omega)_T = \gamma_0 \frac{\omega_0^2 \gamma_0 T}{4\pi^2 c^2 \bar{I}} \sim \gamma_0 \frac{\gamma_0 T}{\lambda_2^2 \bar{I}}. \quad (85)$$

For the values

$$\gamma_0 \sim 25 \text{ s}^{-1}, \quad \lambda_2 \sim 10^{-4} \text{ m}, \quad I \sim 10^{-5} \text{ w/m}^2, \quad kT \sim 3 \cdot 10^{-23} \text{ J}$$

we obtain

$$\frac{(\Delta\omega)_T}{\gamma_0} \sim 10^{-8},$$

which is negligible. In a real experiment there are always other sources of noise except temperature. Estimate (85) determines the condition under which it is necessary to take into account such noise source.

Experimental shape of the second-sound spectrum strongly fluctuates. For good experimental results it can be universally described as a symmetrical spectral line with exponential tails. The width of this spectral line is proportional to  $\epsilon^\alpha$  with  $\alpha \sim 1-1.2$ . This result agrees well with Eqs. (73)–(76).

The results for the intensity of the second-sound waves are not yet fully understood. Experimental values are significantly smaller than theoretical expressions (37) and (38). The reason for this discrepancy is not known. It was shown, in particular, that the intensity of the excited sound wave depends strongly on its shape. The excited second-sound wave in Ref. [5] is not spherical due to the pumping by a standing wave. Unfortunately, experimental information does not allow us to draw definite conclusion about the shape of a parametrically generated sound wave.

## 8. CONCLUSIONS

The theory of parametric excitation of sound waves considered by us differs significantly from the standard theory of spin waves [3]. The most important difference is that three-wave interaction is allowed for sound waves. This three-wave interaction produces nonlinear attenuation of the sound wave and determines the saturated value of the amplitude of an excited wave. The intensity of a parametrically excited sound wave is proportional to the difference between the value of pumping and bare attenuation rate of a sound wave,  $\epsilon = \lambda/\gamma_0 - 1$ .

Three-wave interaction between sound waves is essential only if the angle between their wave vectors is smaller than  $4\sqrt{\gamma_0/\omega}$ . This property destroys long-range order over the angle between waves and accounts for the absence of ordinary pattern formation. The total intensity of a parametrically excited sound wave crucially depends on the shape of the wave. It is maximal for a spherical wave and minimal for a flat wave. The shape of an excited wave is determined by the symmetry of the system (boundary conditions), by the shape of the pumping wave, and by the properties of the interaction vertex between the pumping wave and the sound waves. It is expected that the symmetry of an excited sound wave will be the same as the symmetry of a system due to the peculiar interaction between sound waves.

The spectrum of parametrically excited sound waves is similar to the spectrum of other waves. Thermal broadening of the spectrum is negligible for the experiment in Ref. [6].

Significant broadening of the spectrum of excited waves takes place due to their scattering. The structure of a nonlinear integral equation, which determines the shape of the spectrum of sound waves, is similar to the structure of analogous equations for waves with other dispersion relations. This fact leads to universal shape of the spectrum with exponential asymptotic behavior over the frequency. The width of the spectrum essentially depends on the shape of the wave. Roughly, it is estimated as  $\Delta\omega \sim \gamma_0 \epsilon^\alpha / 4\pi$ . Here  $\gamma_0$  is the bare damping rate of a sound wave, and the value of the parameter  $\alpha$  depends on the shape of the wave. For a flat wave  $\alpha = 1$ , for a cylindrical wave  $\alpha = 8/7$ , and for a spherical wave  $\alpha = 8/6$ , whereas the corresponding index for spin waves is equal to  $2/3$  [3].

I am deeply grateful to V. Lebedev for many useful discussions. I wish to thank D. Rinberg, V. Steinberg, and G. Falkovich for many discussions of the various aspects of the experimental studies [5, 6] and for their hospitality. This work was supported, in part, by the Minerva Center for Nonlinear Physics, INTAS (grant No. 94-4078) and Russian Foundation for Basic Research (grant No. 96-02-18235).

## References

1. M. C. Cross and P. C. Hohenberg, *Rev. Mod. Phys.* **65**, 851 (1993).
2. V. E. Zaharov, V. S. L'vov, and S. Starobinets, *Zh. Eksp. Teor. Fiz.* **59**, 1200 (1970).
3. V. S. L'vov, *Wave Turbulence under Parametric Excitation*, Springer-Verlag, Berlin (1994).
4. W. Zhang and J. Vinals, submitted to *J. Fluid. Mech.*
5. D. Rinberg, V. Cherepanov, and V. Steinberg, *Phys. Rev. Lett.* **76**, 2105 (1996).
6. D. Rinberg, V. Cherepanov, and V. Steinberg, *Phys. Rev. Lett.* **78**, (1997).
7. G. M. Zaslavskii and R. Z. Sagdeev, *Introduction to Nonlinear Physics* [in Russian], Nauka, Moscow (1988).
8. V. L. Pokrovskii and I. M. Khalatnikov, *Zh. Eksp. Teor. Fiz.* **71**, 1974 (1976).
9. H. W. Wyld, *Ann. Phys.* **14**, 143 (1961).
10. C. De Dominicis, *J. de Phys. Colloque* **37**, 247 (1976).
11. H. K. Janssen, *Z. Phys. B* **23**, 377 (1976).
12. E. I. Kats and V. V. Lebedev, *Fluctuational Effects in the Dynamics of Liquid Crystals*, Springer-Verlag, New York (1994).
13. V. V. Lebedev, *Zh. Eksp. Teor. Fiz.* **72**, 2224 (1977).
14. G. Ahlers, in *The Physics of Liquid and Solid Helium*, ed. by K. H. Bennemann and J. B. Ketterson, John Wiley & Sons, New York (1976), p. 85.